Park, J., Kil, H., Stolle, C., Lühr, H., Coley, W. R., Coster, A., Kwak, Y.-S. (2016): Daytime midlatitude plasma depletions observed by Swarm: Topside signatures of the rocket exhaust. - *Geophysical Research Letters*, *43*, 5, pp. 1802—1809.

DOI: http://doi.org/10.1002/2016GL067810

AGU PUBLICATIONS

Geophysical Research Letters

RESEARCH LETTER
10.1002/2016GL067810

Key Points:
- The Swarm detected daytime midlatitude plasma depletions of unknown sources
- Temporal/spatial proximity to rocket launches indicates that they are rocket exhaust depletions
- The characteristics identified by this study can help differentiate natural and man-made phenomena

Correspondence to:
J. Park,
pj@kasi.re.kr

Citation:
Park, J., H. Kil, C. Stolle, H. Lühr, W. R. Coley, A. Coster, and Y.-S. Kwak (2016), Daytime midlatitude plasma depletions observed by Swarm: Topside signatures of the rocket exhaust, *Geophys. Res. Lett.*, *43*, 1802–1809, doi:10.1002/2016GL067810.

Received 16 JAN 2016
Accepted 12 FEB 2016
Accepted article online 18 FEB 2016
Published online 4 MAR 2016

Daytime midlatitude plasma depletions observed by Swarm: Topside signatures of the rocket exhaust

Jaeheung Park[1,2], Hyosub Kil[3], Claudia Stolle[4,5], Hermann Lühr[4], William R. Coley[6], Anthea Coster[7], and Young-Sil Kwak[1,2]

[1]Korea Astronomy and Space Science Institute, Daejeon, Korea, [2]Department of Astronomy and Space Science, University of Science and Technology, Daejeon, Korea, [3]Space Department, Johns Hopkins University Applied Physics Laboratory, Laurel, Maryland, USA, [4]Helmholtz Centre Potsdam GFZ German Research Centre for Geosciences, Potsdam, Germany, [5]Faculty of Science, University of Postdam, Potsdam, Germany, [6]William B. Hanson Center for Space Sciences, University of Texas at Dallas, Richardson, Texas, USA, [7]Haystack Observatory, Massachusetts Institute of Technology, Cambridge, Massachusetts, USA

Abstract The daytime midlatitude plasma depletions (DMLPDs) observed on 22 May 2014 and 20 May 2015 by the Swarm constellation are not explained by any known natural phenomena. The DMLPDs were detected after rocket launches, and the DMLPD traces converged to the launch station. The event in 2015, for which sufficient total electron content (TEC) data are available, is accompanied with TEC depletion lasting for about 6 h. The persistence generally agrees with the lifetime expected for rocket exhaust depletions (REDs) which is determined by the recombination of the ionospheric oxygen ion with water molecules in the rocket exhaust. These results lead to the conclusion that DMLPDs are REDs in the topside. The RED characteristics identified from the observations on both days are (1) enhancement in electron temperature, (2) reduction in electron pressure, and (3) absence of substructures down to scale sizes of about 8 km (Nyquist's scale size).

1. Introduction

Abnormal daytime midlatitude plasma depletions (DMLPDs) were detected over the northern Atlantic Ocean on 22 May 2014 by the Swarm constellation and the Gravity Recovery and Climate Experiment (GRACE) satellite [*Park et al.*, 2015]. The DMLPDs had latitudinal and longitudinal widths of about 300–400 km and 1000 km, respectively. *Park et al.* [2015] tried to explain the DMLPD phenomena in association with some natural phenomena, but they could not clarify the source of the DMLPDs with the limited data set. Similar DMLPDs were detected again over northern Atlantic Ocean on 20 May 2015 by the Swarm constellation. For the events on 20 May 2015, a signature of DMLPDs appeared in the total electron content (TEC) maps. This observation provided a clue for the source of the DMLPDs observed both on 22 May 2014 and 20 May 2015.

In this study, we provide evidence that the DMLPDs observed on 22 May 2014 and 20 May 2015 are man-made phenomena associated with rocket launches. The ionospheric observations of the Swarm and Defense Meteorological Satellite Program (DMSP)/F15 satellites and the TEC maps derived from the Global Navigation Satellite Systems (GNSS) data were used for this study. In section 2, we describe the data sets and rocket launches on the event days. The observation results are presented in section 3. In section 4, we discuss the source and characteristics of the DMLPDs. Conclusions are given in section 5.

2. Data and Rocket Launch Description

An Atlas V Rocket was launched at the Cape Canaveral Air Force Station (28.47°N GLAT, 80.57°W GLON, Florida, U. S.) at 1505 UT on 20 May 2015 (http://www.space.com/29448-x37b-space-plane-launches-fourth-mission.html). On 22 May 2014, the same type of rocket (Atlas V) was launched at the same station at 13:09 UT (http://www.cbsnews.com/news/atlas-5-rocket-launches-with-secret-reconnaisance-satellite/). Unfortunately, the trajectories of those rockets were not available. The levels of solar flux were similar for the two days: the $F_{10.7}$ index was 114 and 108 on 22 May 2014 and 20 May 2015, respectively.

Swarm is the European Space Agency's geomagnetic field mission comprised of three satellites [e.g., *Olsen et al.*, 2013; *Lühr et al.*, 2015]. Each satellite carries magnetometers that measure geomagnetic field vectors

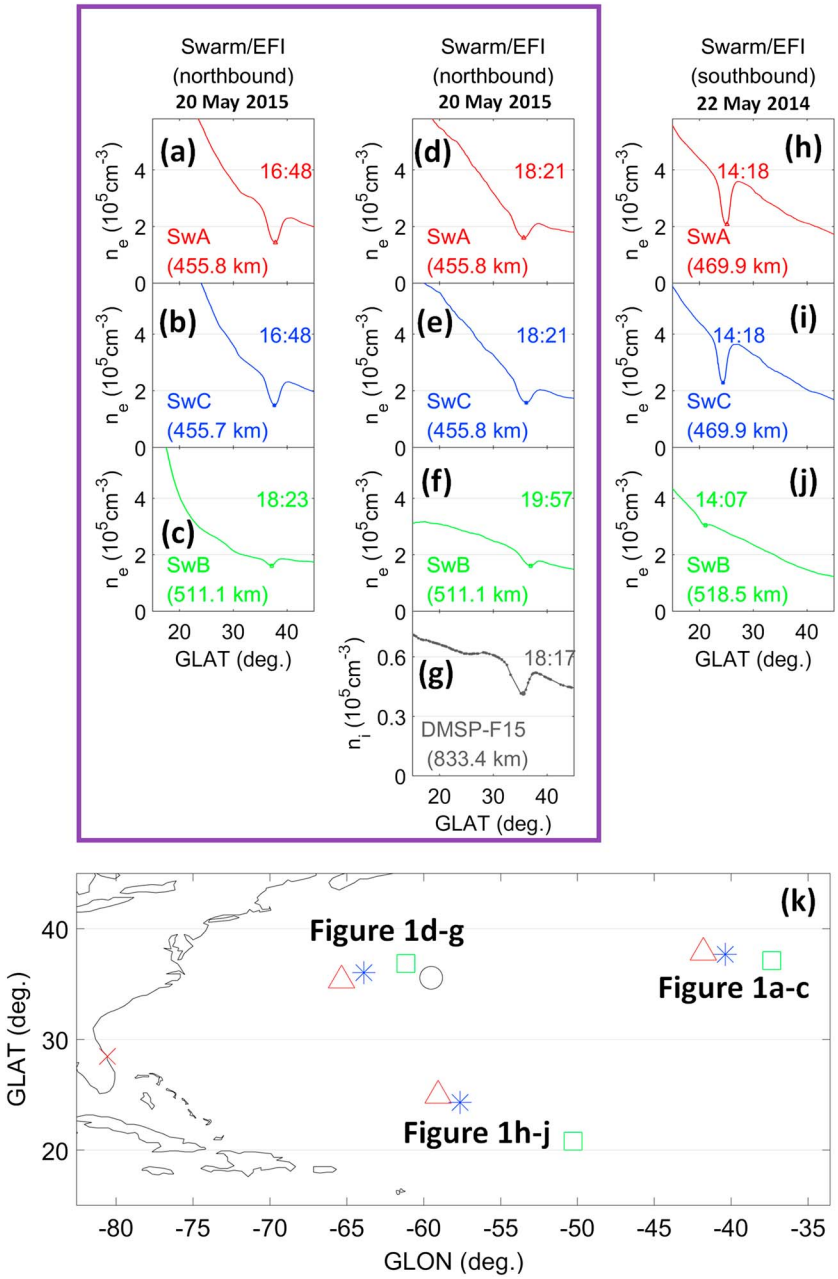

Figure 1. (a–f) Measurements of the electron density along two consecutive orbits of the Swarm constellation on 20 May 2015. (g) Measurements of the ion density by DMSP/F15. (h–j) The same format for the Swarm observations on 22 May 2014. (k) The locations of the DMLPDs observed by Swarm (red/blue/green) and DMSP/F15 (black). The Cape Canaveral Air Force Station in Florida is marked with a red cross.

and Langmuir Probes (LPs) that measure the electron density and temperature [e.g., *Buchert et al.*, 2015]. The two-paired satellites, Swarm-Alpha (SwA) and Swarm-Charlie (SwC) fly side by side at ~470 km altitude with a separation of about 75 km in geographic latitude (GLAT) and about 150 km in geographic longitude (GLON). The stand-alone satellite Swarm-Bravo (SwB) orbits the Earth about 50 km higher than the lower pair. During the event day of our interest (20 May 2015), SwA and SwC detected DMLPDs at around 1400 local time (LT) while SwB detected them around 1600 LT. Our study uses the measurements of the electron density and temperature by the LP. Cross-calibration results between the two LP parameters and independent measurements, which can specify the absolute accuracy of the Swarm/LP data, have not yet been published. Nevertheless, absence of notable small-scale fluctuations (see Figures 1 and 3) suggests that the level of

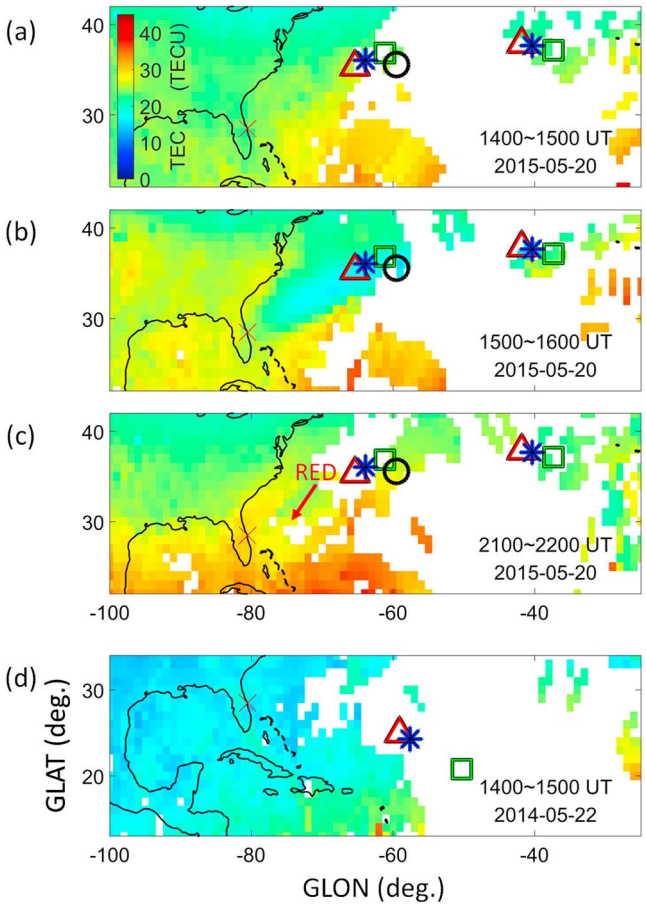

Figure 2. (a–c) Hourly-average TEC maps selected between 1400 and 2000 UT on 20 May 2015 and (d) that for 1400–1500 LT on 22 May 2014. The red/green/blue symbols represent DMLPD events observed by Swarm-Alpha/Bravo/Charlie (also shown in Figure 1), respectively, while the black circle stands for that observed by DMSP/F15.

background noise is much smaller than 10%. In the following sections, therefore, we focus on relative variations of electron density and temperature.

The DMSP spacecraft are a series of Sun-synchronous satellites (http://cindispace.utdallas.edu/DMSP/). The DMSP satellites have circular orbits at the altitude of around 830 km. In this study we use the measurements of the ion density by the DMSP/F15. F15 detected a DMLPD at around 14 LT. We filtered out questionable data points (1) with the retarding potential analyzer flag larger than 2 (representing "caution": refer to http://cindispace.utdallas.edu/DMSP/intro.htm) or (2) with the ion density values staying at a constant value up to the last digit (=0.001 cm^{-3}) for ≥20 s. We believe the latter not being natural but considered it resulting from instrument malfunction. The plasma density of DMSP has an accuracy of about 10% (http://www.dtic.mil/dtic/tr/fulltext/u2/a315731.pdf, Table 3).

Global maps of geodetic median vertical TEC produced using the GNSS data are available at the Haystack Madrigal website (http://madrigal.haystack.mit.edu/madrigal/). The TEC data are provided every 5 min. In this study we use hourly-average TEC maps to acquire sufficient spatial coverage.

3. Results

Figures 1a–1c show the measurements of the electron density by the Swarm/LP. Satellite identifiers and altitudes are given in each figure. DMLPDs were detected around 1648 UT by SwA and SwC and near 1823 UT by SwB. The DMLPD locations of SwA, SwB, and SwC are shown with red, green, and blue symbols, respectively, in Figure 1k. The red cross symbol in Florida indicates the Cape Canaveral Air Force Station.

Figures 1d–1f show the observations on the subsequent Swarm orbits in the same format. The measurements of the ion density by DMSP/F15 are shown in Figure 1g, and the DMLPD detected by F15 is indicated with a

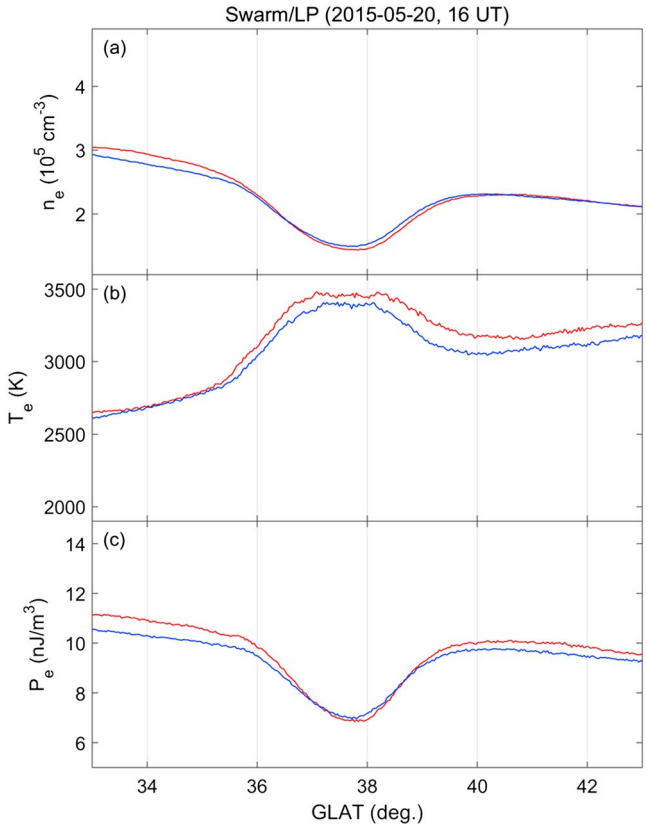

Figure 3. (a) Electron density, (b) electron temperature, and (c) electron pressure obtained from SwA (red) and SwC (blue) around 1648 UT on 20 May 2015.

black circle in Figure 1k. DMLPDs were detected around 18:21 UT by SwA and SwC, near 19:57 UT by SwB, and around 18:17 UT by DMSP/F15. The DMLPDs detected around 18:21 UT by SwA and SwC (Figures 1d and 1e) show deeper plasma depletion than does the DMLPD detected near 18:23 UT by SwB (Figure 1c), although those observations were made at similar UT. Presumably, the SwB orbit was further away from the rocket trajectory than were the other satellite orbits. The difference of the background density at different altitudes may also affect the depletion depth [e.g., *Mendillo et al.*, 1975, equation (25)].

As a reference, the Swarm observations on 22 May 2014 reported *Park et al.* [2015] are presented in Figures 1h–1j. All Swarm observations were made around 14:00 UT (1000 LT). The morphology of the DMLPDs observed on 22 May 2014 is almost identical to that observed on 20 May 2015; the DMLPDs are single trough-like depletions with no internal structure. With the locations of the DMLPDs and rocket launch station in Figure 1k, one may draw trajectories directed north-eastward on 20 May 2015 and south-eastward on 22 May 2014.

Figures 2a–2c present TEC maps over North America and Atlantic Ocean between 1400 and 2200 UT on 20 May 2015. The GLON and GLAT bin sizes in the TEC maps are 1°. The TEC map at 1400–1500 UT (Figure 2a) represents the ionosphere prior to the emergence of DMLPDs. At 1500–1600 UT (Figure 2b), a TEC depletion band that converges to the Cape Canaveral Air Force Station is clearly visible. The locations of the DMLPDs are indicated with the same symbols as in Figure 1. Note that the Atlas V Rocket was launched at 1505 UT on that day. The TEC depletion was persistent even afterward (at least until 2100–2200 UT, Figure 2c).

The TEC map at 1400–1500 UT on 22 May 2014 is shown in Figure 2d. The rocket was launched at 1309 UT on that day. The rocket trajectory is difficult to identify in the TEC map. Significant fluctuations in the background TEC in the time period, coupled with the lack of TEC data at these times, made the identification of the DMLPD signature difficult. Note that the location of the DMLPD observed by GRACE on 22 May 2014 [*Park et al.*, 2015, Figure 3] does not fit well to the line connecting the Cape Canaveral and the Swarm DMLPDs on the same day. As the GRACE DMLPD was much weaker than and temporally separated (by about 6 h) from the

Swarm events, we suspect that the former DMLPD may have a different origin from that of the latter. In the following discussions we omit the GRACE DMLPD on 22 May 2014.

Around 1648 UT on 20 May 2015, when the Swarm satellites observed the most prominent plasma depletions (see Figure 1), the electron temperature is enhanced about 30% at the locations of the plasma depletions (see Figure 3). The product of the electron density and temperature that corresponds to the electron energy density [e.g., *Oyama et al.*, 1988] (or electron pressure) is reduced within the plasma depleted region (see Figure 3). The same properties were identified in the DMLPDs observed on 22 May 2014 [*Park et al.*, 2015]. The DMSP/F15 observations on 20 May 2015 also identified those properties and showed that the oxygen ion fraction did not change much at the location of the DMLPD (figure not shown). We could not detect conspicuous DMLPDs in DMSP data (F15–18) on 22 May 2014 (http://satdat.ngdc.noaa.gov/dmsp/data).

4. Discussion

4.1. Relationship Between DMLPD and RED

The formation of the DMLPDs is difficult to explain in association with any known natural phenomena. The DMLPDs cannot be explained by remnants of nighttime equatorial plasma bubbles [*Park et al.*, 2015]. Medium-scale traveling ionospheric disturbances occur frequently in middle latitudes, but the DMLPDs did not show wave (i.e., multipeaked) characteristics. Other natural disturbances such as geomagnetic storms, tornados, and earthquakes were not recorded on the days and around the locations of the DMLPD detection. Excluding those factors, the DMLPDs are likely man-made phenomena.

The record of rocket launches on the days of the DMLPD detection and the appearance of the DMLPDs after the rocket launches suggest that the DMLPDs observed on 22 May 2014 and 20 May 2015 are related to the rocket exhaust depletions (REDs). This interpretation is supported by the observation of DMLPDs at the location of a TEC depletion band that converges to the rocket launch site. The morphology of the TEC depletion band observed on 20 May 2015 is similar to the morphology of the RED reported by *Mendillo et al.* [2008].

Ionospheric/thermospheric perturbations including REDs produced by rocket launches have been investigated using ionosonde observations [*Booker*, 1961], measurements of airglow emissions [e.g., *Meier et al.*, 2010; *Mendillo et al.*, 2008], and TEC data [*Furuya and Heki*, 2008; *Mendillo et al.*, 2008; *Kakinami et al.*, 2013; *Lin et al.*, 2014; *Nakashima and Heki*, 2014; *He et al.*, 2015]. Those observations represent the phenomena near the *F* region density peak and at lower altitudes. To the best of the authors' knowledge, there have been only a few observational papers about topside signatures of RED, most of which focused only on nighttime events. Using vertical profiles of plasma density reconstructed from Faraday rotation data, *Stone et al.* [1964] investigated RED events for launches during "very late afternoon or evening" hours. The events were shown to straddle the *F* region plasma density peak, sometimes reaching altitudes of about 500 km [e.g., *Stone et al.*, 1964, Figure 8]. *Wand and Mendillo* [1984] used the incoherent scatter radar (ISR) at Millstone Hill (42.6°N GLAT, 71.5°W GLON) for investigating a nighttime RED. Clear RED signatures could be identified between altitudes of 300 km and 500 km [*Wand and Mendillo*, 1984, Plate 1] though the altitude of the rocket-radar beam intersection was only 425 km. *Mendillo et al.* [1987] and *Bernhardt et al.* [1998, 2001] also presented ISR data during rocket launches, but topside signatures of the related RED were not discussed in further detail. The Communications/Navigation Outage Forecasting System (C/NOFS) satellite observed rocket-induced plasma density "enhancement," which was attributed to the "snow plough effect" at the front of the exhaust plume expansion [*Bernhardt et al.*, 2012]. Therefore, the C/NOFS observation of enhanced plasma density was due to the satellite's spatial/temporal (< 1 min after the burn) proximity to the exhaust cloud front: this phenomenon is different from RED resulting from enhanced ion recombination. *Mendillo et al.* [2008] briefly described the detection of a nighttime RED at an altitude of 840 km by DMSP, but the satellite observation data were not shown. In that regard, this study and *Park et al.* [2015] are the first reports on the daytime REDs identified by satellite-based measurements of in situ plasma density.

Assuming that the DMLPDs observed on 22 May 2014 and 20 May 2015 represent REDs, our results provide a complement to existing knowledge of REDs. The observations in this study demonstrate that REDs can last for ≥6 h even during daytime in spite of expected refilling of plasma depletions by photoionization. This event is the most long-lasting dayside RED ever reported. Previous studies reported the persistence of daytime REDs for 0.5–1.5 h [*Booker*, 1961; *Furuya and Heki*, 2008; *Ozeki and Heki*, 2010]. *Mendillo et al.* [1975] reported a daytime RED event that lasted slightly less than 4 h, which is still shorter than the event on 20 May 2015.

Topside signatures of the daytime RED events on 2 days (this study and *Park et al.* [2015]) exhibit no conspicuous horizontal substructure (from the RED scale size of about 300–400 km down to the Nyquist scale

size of about 8 km). The Fresnel scale size of the L1 frequency signals is given by $(2 \times 0.19\ \text{(m)} \times d)^{\frac{1}{2}}$ where d is the irregularity altitude (http://gps.ece.cornell.edu/SpaceWeatherIntro_ed2_10-31-06_ed.pdf). For Swarm-Alpha altitude (~460 km) the Fresnel scale size becomes about 400 m. As the Nyquist scale size of Swarm/LP is about 8 km, which is much larger than the Fresnel scale size (0.4 km), we cannot make a conclusive statement as to whether RED can disturb GNSS signals significantly. Only if we assume decrease of the ionospheric irregularity strength with the decrease of the irregularity scale size, subkilometer scale irregularities (~0.4 km) in REDs may be ignorable. Previous ground-based observations have reported somewhat conflicting results about the substructure and loss of communication. *Mendillo et al.* [2008] reported a brief loss of lock in the GNSS signals around a nighttime RED. In some other cases, ground radio receivers did not observe scintillations near RED events during daytime [*Mendillo et al.*, 1975] or nighttime [*Mendillo et al.*, 1980]. A nighttime RED reported by *Mendillo et al.* [1980] did not exhibit substructures at scale sizes >1 km (but smaller than the RED size). Note that *Lin et al.* [2014] reported the observation of wave-like disturbances in TEC that propagated rapidly (about 1 km/s) away from a rocket trajectory. Those disturbances were associated with shock/bow waves, and therefore, they are different from REDs which are nearly stationary [*Mendillo et al.*, 2008, Figure 2] and produced by chemical reactions.

For the topside daytime REDs, the electron temperature and electron pressure inside the REDs were higher and lower, respectively, than those of ambient plasma. *Kakinami et al.* [2011, Figure 1] showed that electron temperature in the daytime midlatitude topside is generally anticorrelated with electron density, which agrees with our results. *Park et al.* [2015] suggested that the higher (lower) electron temperature inside (outside) the DMLPD result from heating by photoelectrons which are energetic electrons that are directly produced through photoionization of the neutral gas. The loss rate of photoelectrons is approximately quadratic in ion density [*Stolle et al.*, 2011, and references therein], thus cooling by ions is increased outside the depletion. The anticorrelation between electron density and temperature breaks at dayside equatorial latitudes near the altitudes of Swarm [*Kakinami et al.*, 2011, Figure 2]. But the REDs discussed here are clearly outside the equatorial latitudes.

4.2. Comparison With Theoretical Estimations

4.2.1. Lifetime

The RED event analyzed by *Mendillo et al.* [1975] occurred near the Cape Canaveral Air Force Station in Florida near 1730 UT on 14 May 1973 ($F_{10.7} = 89.3$). The ambient conditions of that event were similar to those of the RED event on 20 May 2015: in respect of the rocket trajectory (*Mendillo et al.* [1975] Figure 3 versus Figure 2 in this study), day of year (134 versus 140), rocket launch time (1730 UT versus 1505 UT), and $F_{10.7}$ (89.3 versus 108). The D_{st} index (http://wdc.kugi.kyoto-u.ac.jp/dstdir/index.html) was −62 nT at 1730 UT on 14 May 1973 and −18 nT at 1505 UT on 20 May 2015. Therefore, we make use of the physics equations and reaction coefficients used by *Mendillo et al.* [1975] in order to estimate RED properties theoretically. In this study we only conduct order of magnitude estimations. More accurate three-dimensional (3-D) modeling would require detailed information on the rocket trajectory and amount of the released exhaust, which is left for future studies.

According to *Mendillo et al.* [1975, equation (25)] the continuity equation of TEC is:

$$\frac{\partial N_{\text{TEC}}}{\partial t} = q - \beta_{\text{eff}} \times N_{\text{TEC}} + M, \tag{1}$$

where N_{TEC} is TEC, q and β_{eff}, respectively, represent production and loss coefficients under quiet conditions (i.e., in the absence of rocket exhaust), and M signifies contribution from the divergence of plasma motion. Following *Mendillo et al.* [1975], we assume that rocket exhaust only changes β_{eff}, while q and M remain intact. Then, we can estimate $q + M$ using TEC data before the rocket launch [*Mendillo et al.*, 1975]. Note that background TEC (N_{TEC}) at 14–15 UT was about 25 total electron content unit, 1 TECU = 10^{16} el m^{-2} near the upcoming RED trajectory (see Figure 2a) and that the prelaunch natural TEC change from 13–14 UT (figure not shown) to 14–15 UT is of the order of 1 TECU: i.e., 1 TECU change during 3600 s. With the quiet time β_{eff} of about 2×10^{-5} s^{-1} [*Mendillo et al.*, 1975, equation (10)], we obtain

$$\begin{aligned} q + M &= \frac{\partial N_{\text{TEC}}}{\partial t} + \beta_{\text{eff}} \times N_{\text{TEC}} \\ &\approx \left[\frac{1\ \text{(TECU)}}{3600\ \text{(s)}} + 2 \times 10^{-5}\ (\text{s}^{-1}) \times 25\ \text{(TECU)} \right] \\ &\approx 8 \times 10^{-4}\ \text{(TECU/s)}. \end{aligned} \tag{2}$$

After rocket launch the loss coefficient in the continuity equation (β_{eff}) becomes higher (β_{RED}):

$$\frac{\partial N_{TEC}}{\partial t} = q + M - \beta_{RED} \times N_{TEC} \approx 8 \times 10^{-4}\,(\mathrm{TECU/s}) - \beta_{RED} \times N_{TEC}. \quad (3)$$

This equation controls the lifetime (or refilling time) of RED. The first term on the right-hand side is photoionization and transport ($q + M$) by quiet time ionospheric processes, and the second term (enhanced recombination loss due to rocket exhaust) prevents RED from refilling. We assume an extreme case of no recombination ($\beta_{RED} = 0$), which would result in fastest disappearance of RED. In Figure 2b the TEC inside and outside the RED is about 20 TECU and 25 TECU, respectively. Therefore, the time needed for the RED (20 TECU) to get additional 5 TECU (i.e., refilling) by photoionization and transport is approximated by

$$\begin{aligned} \Delta t &\approx \frac{\Delta N_{TEC}}{8 \times 10^{-4}\,(\mathrm{TECU/s})} \\ &\approx \frac{5\ (\mathrm{TECU})}{8 \times 10^{-4}\,(\mathrm{TECU/s})} \\ &\approx 6250(\mathrm{s}) \approx 1.7(\mathrm{hours}). \end{aligned} \quad (4)$$

Now we reconsider the enhanced recombination (β_{RED}). From *Mendillo et al.* [1975, Figure 8c] we can estimate β_{RED} to be approximately between 2×10^{-6} s^{-1} and 2×10^{-2} s^{-1}: exact values depend on, for example, the amount of exhaust, distance from the rocket trajectory, and time elapsed from the exhaust release. Within 500 km from the rocket trajectory the β_{RED} stays above 3×10^{-5} s^{-1} even 2 h after the exhaust release [*Mendillo et al.*, 1975, Figure 8c]. Assuming that this level of recombination persists for several hours, the time needed for the RED to get additional 5 TECU (i.e., refilling; see Figure 2) under photoionization, transport, and rocket exhaust can be approximated by the following equation:

$$\begin{aligned} \Delta t &\approx \frac{\Delta N_{TEC}}{8 \times 10^{-4} - 3 \times 10^{-5} \times 20\,(\mathrm{TECU/s})} \\ &\approx \frac{5(\mathrm{TECU})}{2 \times 10^{-4}\,(\mathrm{TECU/s})} \\ &\approx 25000(\mathrm{s}) \approx 7(\mathrm{hours}). \end{aligned} \quad (5)$$

Therefore, the lifetime of about 6 h as shown in Figure 2 has an order of magnitude consistent with the theoretical estimates following *Mendillo et al.* [1975].

4.2.2. Oxygen and Hydrogen Fraction

There was no notable change in the oxygen ion fraction inside the RED on 20 May 2015: it stayed around 96%. This result is intriguing because previous papers [e.g., *Mendillo et al.*, 1975, equations (11)–(12)] generally attributed RED to oxygen ion loss promoted by rocket exhaust plumes. In this subsection we discuss the reason for the insignificant changes in the oxygen ion fraction. First, we assume that water molecules are the dominant component of rocket exhaust, as is in the case investigated by *Mendillo et al.* [1975, p. 2222]. According to *Bernhardt et al.* [2001, p. 1212] the net reaction between water molecules and ionospheric oxygen ion can be expressed as

$$O^+ + e^- + H_2O \rightarrow OH + H + O. \quad (6)$$

This reaction produces equal numbers of neutral hydrogen and oxygen atoms. Following *Waldrop et al.* [2006, equation (4)] the equilibrium state of the $O^+ - H$ and $O - H^+$ charge exchange reactions is represented by the following equation:

$$\frac{[O]}{[H]} \propto \frac{[O^+]}{[H^+]}. \quad (7)$$

As water molecules produce equal number of oxygen and hydrogen fractions, the $[O^+]$ depletion by water molecules may not change the ratio between [O] and [H] drastically. In consequence, in an equilibrium state of the charge exchange, the ratio between $[O^+]$ and $[H^+]$ cannot exhibit revolutionary changes. Also note that the H^+ loss by the charge exchange with O has the reaction coefficient of about 1×10^{-9} cm^3 s^{-1} [*Waldrop et al.*, 2006, Figure 1]. The value is comparable to that of the fast loss that $[O^+]$ experiences in the presence of water molecules [see *Mendillo et al.*, 1975, equations (13)–(15); *Bernhardt et al.*, 2012, Table 1]. Therefore, time scale of the former reaction (charge exchange loss of $[H^+]$) is expected to be similar to that of the latter ($[O^+]$ loss by water molecules in the rocket exhaust). We suggest that the fast charge exchange is the main mechanism to keep the oxygen ion fraction nearly constant in spite of the fast loss of oxygen ions by water molecules.

5. Conclusion

Daytime midlatitude plasma depletions (DMLPDs) were observed on 22 May 2014 by the Swarm constellation [*Park et al.*, 2015], but their source was not clarified at that time because of the lack of extensive supporting observations. Similar phenomena were observed on 20 May 2015 by the Swarm constellation and DMSP/F15 satellite. On both days, DMLPDs were detected a few hours after rocket launches at the Cape Canaveral Air Force Station in Florida. The GNSS TEC maps on 20 May 2015 exhibit the development of a TEC depletion band within an hour after the Atlas V rocket launch and the convergence of the TEC depletion band to the rocket launch site. These facts strongly suggest that the DMLPDs observed on 20 May 2015 were associated with the rocket launch. Though the event is the most long-lasting (lifetime ~6 h) dayside RED event ever reported, its lifetime is still of the right order of magnitude expected by the theoretical estimations following *Mendillo et al.* [1975]. The observed insensitivity of oxygen ion fraction to RED is also as expected from the charge exchange equilibrium between oxygen-hydrogen atoms and ions [*Waldrop et al.*, 2006]. As the DMLPD properties and the background conditions on 22 May 2014 are similar to those of 20 May 2015, the former DMLPDs are also interpreted to be the topside signature of the RED.

Acknowledgments

The authors thank W. K. Lee for her valuable comments on data processing. The European Space Agency (ESA) is acknowledged for providing the Swarm data via https://earth.esa.int/web/guest/swarm/data-access. Global maps of geodetic median Vertical Total Electron Content (VTEC) are available at the Haystack Madrigal Site (http://madrigal.haystack.mit.edu/madrigal/). GPS TEC data products and access through the Madrigal distributed data system are provided to the community by the Massachusetts Institute of Technology under support from US National Science Foundation grant AGS-1242204. Data for the TEC processing are provided from the following organizations: UNAVCO, Scripps Orbit and Permanent Array Center, Institut Geographique National, France, International GNSS Service, The Crustal Dynamics Data Information System (CDDIS), National Geodetic Survey, Instituto Brasileiro de Geografia e Estatstica, RAMSAC CORS of Instituto Geogr?fico Nacional del la Rep?blica Agentina, Arecibo Observatory, Low-Latitude Ionospheric Sensor Network (LISN), Topcon Positioning Systems, Inc., Canadian High Arctic Ionospheric Network, Institute of Geology and Geophysics, Chinese Academy of Sciences, China Meterorology Administration, Centro di Ricerche Sismogiche, Syst?me d'Observation du Niveau des Eaux Littorales (SONEL), RENAG : REseau NAtional GPS permanent, and GeoNet - the official source of geological hazard information for New Zealand. The DMSP data are partly available at http://satdat.ngdc.noaa.gov/dmsp/data. J. Park was supported by the "Planetary system research for space exploration" project, the basic research funding from KASI, and the Air Force Research Laboratory, under agreement number FA2386-14-1-4004. H. Kil acknowledges the support by the National Science Foundation aeronomy program (AGS-1237276) and Wright-Patterson Air Force Base. All data used for this study are available by contacting J. Park (pj@kasi.re.kr).

References

Bernhardt, P. A., J. D. Huba, W. E. Swartz, and M. C. Kelley (1998), Incoherent scatter from space shuttle and rocket engine plumes in the ionosphere, *J. Geophys. Res.*, *103*(A2), 2239–2251, doi:10.1029/97JA02866.

Bernhardt, P. A., J. D. Huba, E. Kudeki, R. F. Woodman, L. Condori, and F. Villanueva (2001), Lifetime of a depression in the plasma density over Jicamarca produced by space shuttle exhaust in the ionosphere, *Radio Sci.*, *36*(5), 1209–1220, doi:10.1029/2000RS002434.

Bernhardt, P., et al. (2012), Ground and space-based measurement of rocket engine burns in the ionosphere, *IEEE Trans. Plasma Sci.*, *40*(5), 1267–1286.

Booker, H. G. (1961), A local reduction of *F*-region ionization due to missile transit, *J. Geophys. Res.*, *66*(4), 1073–1079, doi:10.1029/JZ066i004p01073.

Buchert, S., F. Zangerl, M. Sust, M. André, A. Eriksson, J. Wahlund, and H. Opgenoorth (2015), SWARM observations of equatorial electron densities and topside GPS track losses, *Geophys. Res. Lett.*, *42*, 2088–2092, doi:10.1002/2015GL063121.

Furuya, T., and K. Heki (2008), Ionospheric hole behind an ascending rocket observed with a dense GPS array, *Earth Planets Space*, *60*, 235–239.

He, L. M., L. X. Wu, S. J. Liu, and S. N. Liu (2015), Superimposed disturbance in the ionosphere triggered by spacecraft launches in China, *Ann. Geophys.*, *33*, 1361–1368, doi:10.5194/angeo-33-1361-2015.

Kakinami, Y., S. Watanabe, J.-Y. Liu, and N. Balan (2011), Correlation between electron density and temperature in the topside ionosphere, *J. Geophys. Res.*, *116*, A12331, doi:10.1029/2011JA016905.

Kakinami, Y., M. Yamamoto, C.-H. Chen, S. Watanabe, C. Lin, J.-Y. Liu, and H. Habu (2013), Ionospheric disturbances induced by a missile launched from North Korea on 12 December 2012, *J. Geophys. Res. Space Physics*, *118*, 5184–5189, doi:10.1002/jgra.50508.

Lin, C. H., J. T. Lin, C. H. Chen, J. Y. Liu, Y. Y. Sun, Y. Kakinami, M. Matsumura, W. H. Chen, H. Liu, and R. J. Rau (2014), Ionospheric shock waves triggered by rockets, *Ann. Geophys.*, *32*, 1145–1152, doi:10.5194/angeo-32-1145-2014.

Lühr, H., J. Park, J. W. Gjerloev, J. Rauberg, I. Michaelis, J. M. G. Merayo, and P. Brauer (2015), Field-aligned currents' scale analysis performed with the Swarm constellation, *Geophys. Res. Lett.*, *42*, 1–8, doi:10.1002/2014GL062453.

Meier, R. R., J. M. C. Plane, M. H. Stevens, L. J. Paxton, A. B. Christensen, and G. Crowley (2010), Can molecular diffusion explain Space Shuttle plume spreading?, *Geophys. Res. Lett.*, *37*, L08101, doi:10.1029/2010GL042868.

Mendillo, M., G. S. Hawkins, and J. A. Klobuchar (1975), A sudden vanishing of the ionospheric *F* region due to the launch of Skylab, *J. Geophys. Res.*, *80*(16), 2217–2228, doi:10.1029/JA080i016p02217.

Mendillo, M., D. Rote, and P. A. Bernhardt (1980), Preliminary report on the HEAO hole in the ionosphere, *Eos Trans. AGU*, *61*(28), 529–529, doi:10.1029/EO061i028p00529.

Mendillo, M., J. Baumgardner, D. P. Allen, J. Foster, J. Holt, G. R. A. Ellis, A. Klekociuk, and G. Reber (1987), Spacelab-2 plasma depletion experiments for ionospheric and radio astronomical studies, *Science*, *238*, 1260–1264, doi:10.1126/science.238.4831.1260.

Mendillo, M., S. Smith, A. Coster, P. Erickson, J. Baumgardner, and C. Martinis (2008), Man-made space weather, *Space Weather*, *6*, S09001, doi:10.1029/2008SW000406.

Nakashima, Y., and K. Heki (2014), Ionospheric hole made by the 2012 North Korean rocket observed with a dense GNSS array in Japan, *Radio Sci.*, *49*, 497–505, doi:10.1002/2014RS005413.

Olsen, N., et al. (2013), The swarm satellite constellation application and research facility (SCARF) and swarm data products, *Earth Planets Space*, *65*(11), 1189–1200.

Oyama, K.-I., K. Schlegel, and S. Watanabe (1988), Temperature structure of plasma bubbles in the low latitude ionosphere around 600 km altitude, *Planet. Space Sci.*, *36*(6), 553–567.

Ozeki, M., and K. Heki (2010), Ionospheric holes made by ballistic missiles from North Korea detected with a Japanese dense GPS array, *J. Geophys. Res.*, *115*, A09314, doi:10.1029/2010JA015531.

Park, J., C. Stolle, C. Xiong, H. Lühr, R. F. Pfaff, S. Buchert, and C. R. Martinis (2015), A dayside plasma depletion observed at midlatitudes during quiet geomagnetic conditions, *Geophys. Res. Lett.*, *42*, 967–974, doi:10.1002/2014GL062655.

Stolle, C., H. Liu, V. Truhlík, H. Lühr, and P. G. Richards (2011), Solar flux variation of the electron temperature morning overshoot in the equatorial *F* region, *J. Geophys. Res.*, *116*, A04308, doi:10.1029/2010JA016235.

Stone, M. L., L. E. Bird, and M. Balser (1964), A Faraday rotation measurement on the ionospheric perturbation produced by a burning rocket, *J. Geophys. Res.*, *69*(5), 971–978.

Wand, R. H., and M. Mendillo (1984), Incoherent scatter observations of an artificially modified ionosphere, *J. Geophys. Res.*, *89*(A1), 203–215, doi:10.1029/JA089iA01p00203.

Waldrop, L. S., E. Kudeki, S. A. González, M. P. Sulzer, R. Garcia, M. Butala, and F. Kamalabadi (2006), Derivation of neutral oxygen density under charge exchange in the midlatitude topside ionosphere, *J. Geophys. Res.*, *111*, A11308, doi:10.1029/2005JA011496.